

# The influence of Bit Error Rate on four-channel Wavelength Division Multiplexing system with the channel spacing of 4 nm in C band with the speed of 10 Gbps and three different pumping powers in an optical fibre amplifier of 980 nm

PETR IVANIGA<sup>1</sup>, TOMÁŠ IVANIGA<sup>2</sup>

1) Department of Information Networks

Faculty of Management Science and Informatics, University of Žilina

Univerzitná 8215/1, 010 26, Žilina

SLOVAKIA

2) Department of Electronic and Multimedia Communications

Faculty of Electrical Engineering and informatics, University of Technology Košice

Park Komenského 13, 041 20, Košice

SLOVAKIA

petr.ivaniga@fri.uniza.sk, tomas.ivaniga@tuke.sk

*Abstract:* - This article focuses on the simulation of four-channel WDM (Wavelength Division Multiplexing) system with the spacing of 4 nm and the speed of 10 Gbps. It underlines the error rate BER (Bit Error Rate) which changes with the input power of fibre amplifier EDFA (Erbium Doped Fibre Amplifier) for the respective channel of WDM. Nowadays while designing the WDM it cannot be done without software tools simulating a real network to avoid possible mistakes which could occur before the actual construction of communication systems. Simulation solves the creation of WDM from 1554 to 1566 nm with the best error rate for the respective channel using single-mode optical fibre 40 km long with measurable attenuation constant according to ITU-T G-652-D.

*Key-Words:* - Bit Error Rate, Erbium Doped Fibre Amplifier, Q-factor, Wavelength Division Multiplexing

## 1 Introduction

Nowadays in terms of the working range financial costs of the wavelengths and generated profit the most suitable optical amplifier for WDM systems is the EDFA amplifier formed by the doped ions  $\text{Er}^{3+}$ . These ions have the ability to absorb radiation in the spectrum around a wavelength of 1550 nm [1], [2], [3], [6], [7]. The amplifier requires pumping the wavelength of 980 nm to connect the input of a laser operating at this wavelength. The technology amplifiers for erbium base doped fibre are used for WDM systems [4], [5]. Their task is to amplify all the WDM channels at once and without the change of optical signal into electrical signal and back. The second chapter describes the EDFA principle and the connection for WDM systems. The third chapter deals with the BER and Q - factor and their mutual dependency. The last chapter is the simulation representing the WDM with EDFA for the means of

comparison of BER and Q-factor. The last chapter summarizes the results obtained from these simulations and describes the best error rate conforming to the channel with the given EDFA power.

## 2 The EDFA principle

Due to bound radiation from the pump laser (at a wavelength of 980 nm or 1480 nm) into the special fibre with a length of several meters (about 10 meters), a carbon doped element excitation happens - in this case erbium ions  $\text{Er}^{3+}$ . The absorbed energy enables the transition to a higher energy level E3 [6], [9]. In this so-called metastable state the ions remain for a very short time (several milliseconds) [8]. This is followed by non-radioactive transition to the E2 levels in the conduction band. After reaching population inversion state, when the majority of

erbium ions are in an excited state, due to the presence of the transmitted signal the energy is released [2], [5], [6].

Following the return of the excited ions to the basic energy level E1 in the valence band accompanied by stimulated emission of radiation of the same wavelength and phase of the transmitted signal. This temporarily stores the energy obtained from the pump laser radiation. It amplifies transmitted optical signal at a wavelength of 1550 nm. During amplification the noise is amplified in the amplified band and spontaneous emission processes intensify (the natural transition of an electron to a lower level). The amplification transmits optical signal at a wavelength of 1550 nm. Fig.1 illustrates the excitation of atoms due to erbium pumping radiation emission [7], [9].

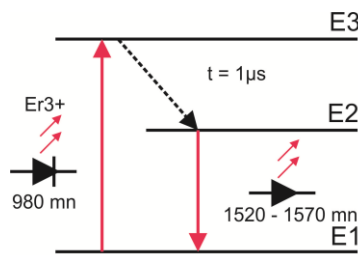


Fig. 1: The erbium excitation as a result of pumping radiation emission.

## 2.1 The EDFA connection

The optical amplifiers operate on the principle of stimulated emission of radiation for amplifying the input optical signal. The operating principle is very similar to the way lasers work. For generating new photons an amplifier has to be connected to the optical pump. This energy is either supplied by an electric field by a semiconductor amplifier or using pump radiation in the fibre amplifiers. With amplification a spontaneous emission noise can also occur (the natural transition of an electron to a lower level) called ASE (Amplified Spontaneous Emission). The EDFA is formed by a laser radiation source called a laser pump and a special optical fibre which is doped with erbium. Due to radiation from the laser pump the profit is generated in the telecom C band. The generated radiation is added to

the signal in this band transmitting data [3], [4], [8], [9]. Fig. 2 shows a circuit diagram of the EDFA.

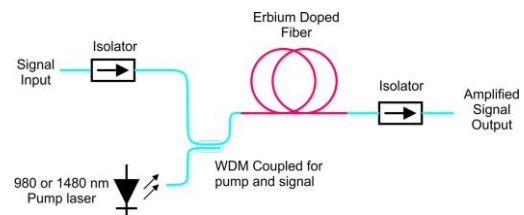


Fig. 2: The scheme of the EDFA connection.

For ensuring the optimal noise characteristics the EDFA amplifiers operate just below the saturation level. This reduces the spontaneous emission in the doped fibre and also noise and ASE [9].

## 3 BER and Q-Factor

BER is characteristic, very useful for finding out a system performance [10]. BER parameter describes the ratio between bits wrongly detected and a total number of bits received (transmitted) [11]. As we can see in Fig. 3, there are two regions, P (1/0) and P (0/1), needed to be discussed in detail. The information is detected in two levels, 0 and 1. These two levels have corresponded with current values  $I_0$ ,  $I_1$  as well as their variances  $\sigma_0$ ,  $\sigma_1$ . The variances have usually different values. If the incoming signal has a value within  $\sigma_1$ ,  $I_1$  region "1" is detected, the analogical process is applied with "0" level detection. However sometimes system makes an error and "0" is recognized when "1" was transmitted to P(0/1), as shown in Fig.3 (a lower region) [12], [13].

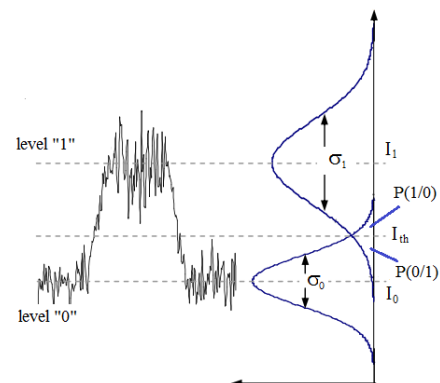


Fig. 3: Probability of a detection P(1/0) and P(0/1) with corresponding variances for level 1 and level 2 at the receiver end.

Complementary “1” can be detected when “0” was sent to P(1/0) (a upper region) [15]. Corresponding probability functions are defined as follows:

$$P(0/1) = \frac{1}{\sqrt{2\pi}\sigma_1} \int_{-\infty}^{I_{th}} e^{-\frac{(I-I_1)^2}{2\sigma_1^2}} dI, \quad (1)$$

$$P(1/0) = \frac{1}{\sqrt{2\pi}\sigma_0} \int_{I_{th}}^{\infty} e^{-\frac{(I-I_0)^2}{2\sigma_0^2}} dI. \quad (2)$$

The next step is to define some complementary error functions for P(0/1) and P(1/0):

$$P(0/1) = \frac{1}{2} \operatorname{erfc}\left(\frac{I_1 - I_{th}}{\sigma_1 \sqrt{2}}\right), \quad (3)$$

$$P(1/0) = \frac{1}{2} \operatorname{erfc}\left(\frac{I_{th} - I_0}{\sigma_0 \sqrt{2}}\right). \quad (4)$$

BER has the minimum value when P(0/1) and P(1/0) regions are equal [14], [17]. From this assumption we have to set the following condition for a threshold current  $I_{th}$  which is important to be set correctly [16]:

$$\frac{I_1 - I_{th}}{\sigma_1} = \frac{I_{th} - I_0}{\sigma_0} \Rightarrow I_{th} = \frac{\sigma_0 I_1 + \sigma_1 I_0}{\sigma_1 + \sigma_0}. \quad (5)$$

Now we can define another parameter called Q – factor, shown in equation:

$$Q = \frac{I_1 - I_0}{\sigma_1 + \sigma_0}. \quad (6)$$

Q – factor describes the margin between two levels, “0” and “1”, and their relation to the corresponding variances  $\sigma_1, \sigma_2$  [18], [19], [20]. By assuming that BER is a sum of the regions shown in equations (3,4) we can define the following equation [21]:

$$BER = \frac{1}{4} \left\{ \operatorname{erfc}\left(\frac{I_1 - I_{th}}{\sigma_1 \sqrt{2}}\right) + \operatorname{erfc}\left(\frac{I_{th} - I_0}{\sigma_0 \sqrt{2}}\right) \right\}. \quad (7)$$

Now it is possible to write a final equation for BER as well as its approximation by using exponential function as shown in the following equation [22], [23]:

$$BER = \frac{1}{2} \operatorname{erfc}\left(\frac{Q}{\sqrt{2}}\right) \approx \frac{e^{-\frac{Q^2}{2}}}{Q\sqrt{2\pi}}. \quad (8)$$

#### 4 The simulation of four-channel WDM system with two pumping EDFA performances (0.01 W, 0.035 W, 0.5 W) at a speed of 10 Gbps per channel from 1554 to 1566 nm

For simulating eye diagram and EDFA spontaneous emission was created a topology of a four-channel WDM system (with a channel spacing of 4 nm) was generated. Fig. 4 shows the topology of a WDM system created with OptSim.

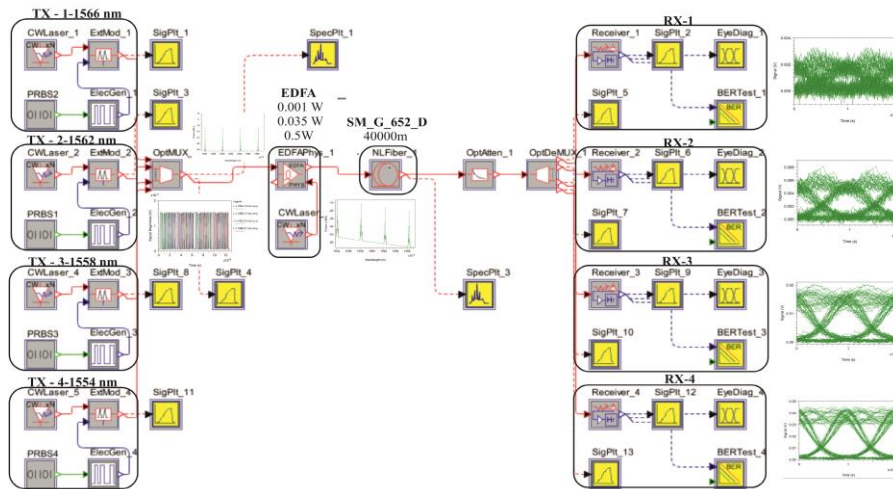


Fig. 4: The topology of a four-channel WDM system.

The whole topology consists of four transmitters (TX-1, TX-2, TX-3, TX-4) of the transmitting part and four receivers (RX-1, RX-2, RX-3, RX-4). Each TX includes: CW laser, an external modulator, an electric signal generator and data source (PRBS). PRBS has a set bit rate at 10 Gbps. CW lasers have set peak power at 0.01 W. The electric generator is used by the modulation format type Non Return to Zero (NRZ) with a filter type Ring Filter. The last component in the transmitter is an external modulator that uses modulation type MachZehnder. Fig. 5 shows the output of the transmitting part of the optical multiplexor.

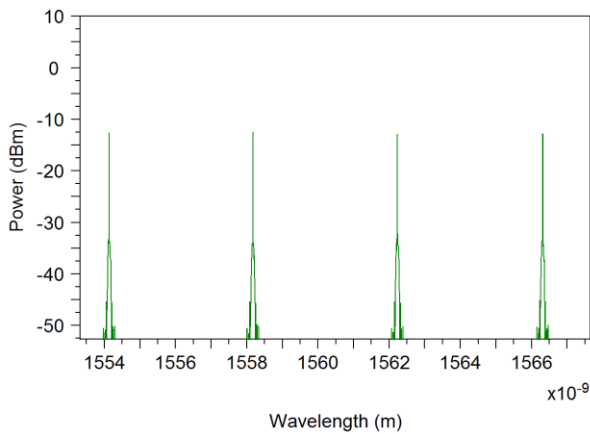


Fig. 5: The output of the transmitting part.

Behind the transmitting part is the transferring part consisting of: optical multiplexor, optical demultiplexor, EDFA, optical fibre, CW laser and a component for the attenuation of the transmitted route. All signals enter the optical multiplexor which uses the Trapezoidal filter and is set to 3dB. Table 1 offers values of the four receivers as the output for the optical multiplexor.

Table 1: Values of four transmitters used

	TX1	TX2	TX3	TX4
Wavelength[nm]	1566	1562	1558	1554
Frequency [THz]	191399	191899	192399	192900
Average [dBm]	-	-	-	-
Pattern length [bits]	128			
Time step [s]	3.125e-12			
Bitrate [bps]	10000000000			

The overall output of the optical multiplexor is - 5.0998 dBm. During simulations we used single-

mode optic fibre according to the standard in ITU-T G-652-D, length of 40 000 m with measurable attenuation constant of 0.3 dB/km. Optical attenuation of the transmission part was set to constant -5 dB. We also used optical amplifier EDFA with 3 pump powers by CW laser with the powers of: 0.01 W, 0.035 W a 0.5 W. In Fig.6 the influence of the spontaneous emission can be observed within the testing regime of EDFA.

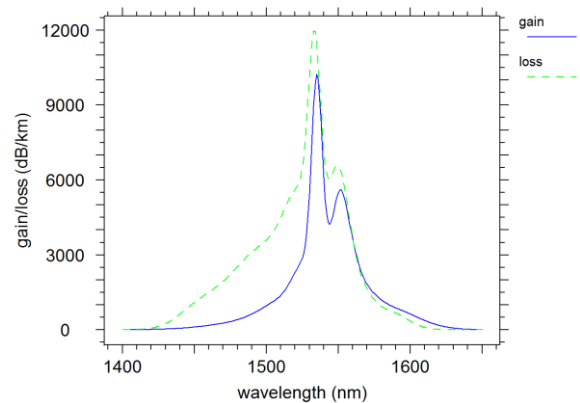


Fig. 6: The influence of the spontaneous emission EDFA.

In Fig. 7 we can see the optical spectrum of the EDFA amplification at a wavelength of 980 nm with a three different pumping powers: 0.01 W, 0.035 W, 0.5 W.

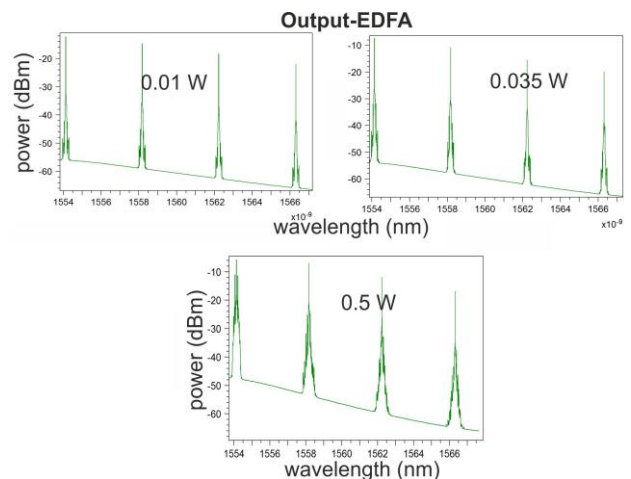


Fig. 7: The EDFA output for various performances (0.01 W, 0.035 W, 0.5 W).

The EDFA internal processes with various input powers are shown in detail in Fig. 8. In it we can see the input signal increase while retaining the EDFA

length. The dependence of the ASE effect on the output of CW laser is shown in Fig. 8.

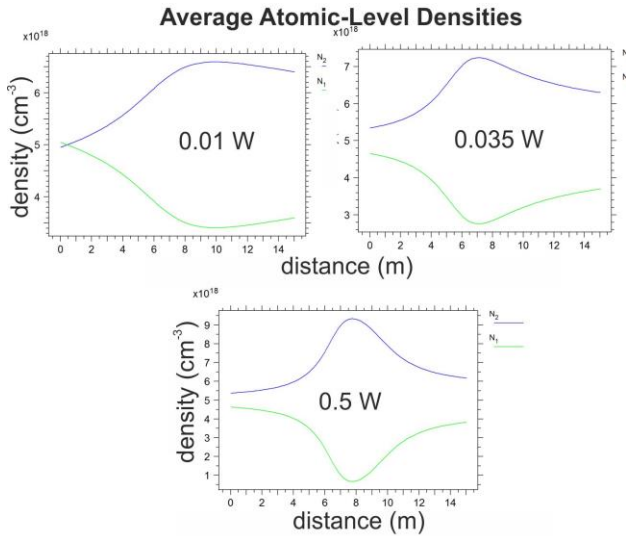


Fig. 8: The density state of erbium with various powers (0.01 W, 0.035 W, 0.5W) and constant length.

The ASE noise is approximately eliminated in proportion to the increasing input signal. The higher value (input) activates (excites) more erbium to a significant amplification. The smaller part of the erbium is therefore used to amplify spontaneous emission and can be seen in Fig 9.

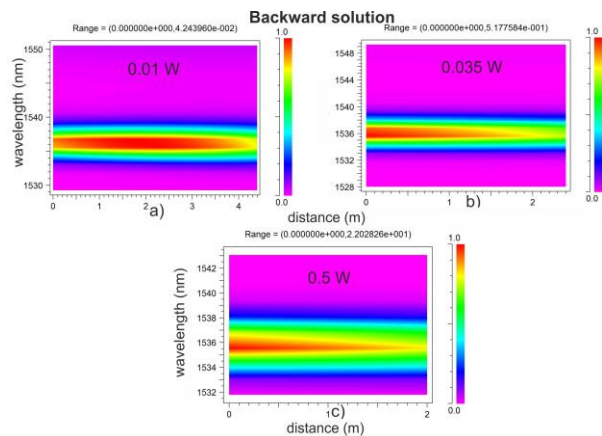


Fig. 9: The ASE spread with various input powers (0.01 W, 0.035 W, 0.5 W).

At the end of the transmission part is the optical demultiplexor which uses Trapezoidal filter with attenuation of 3 dB. In Table 2 are the output values of the amplifier entering the optical demultiplexor.

Table 2: The output values of the amplifier

	TX1	TX2	TX3	TX4
<b>Wavelength[nm]</b>	1.566	1.562	1.558	1.554
<b>Frequency[THz]</b>	191399	191899	192399	192900
<b>Average [dBm]</b>				
0.01W	-25.343	-21.641	-18.091	-15.532
0.035W	-23.141	-18.6620	-13.9666	-10.1850
0.5W	-19.752	-14.4043	-8.35280	-3.02854
<b>Peak noise density[dBm/Hz]</b>				
0.01W	-127.55477769521026			
0.035W	-119.99091182624034			
0.5W	-106.54101404945537			
<b>Total average power [dBm]</b>				
0.01W	-12.735420576736415			
0.035W	-8.1133573717968908			
0.5W	-1.6059468267977888			
<b>Pattern length [bits]</b>	128			
<b>Time step [s]</b>	3.125e-12			
<b>Bitrate [bps]</b>	10000000000			

The receiving part consists of a PIN photodiode, preamplifier and Bessel filter connected to one component. Fig 10 shows the eye diagrams for the receiver No.1 with EDFA input powers: 0.01 W, 0.035 W, 0.5 W. In Table 3 are the output values for the receiver #1.

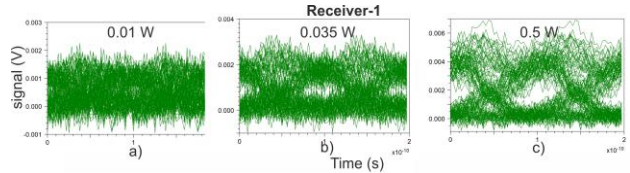


Fig. 10: The eye diagrams for the receiver #1 with powers (0.01 W, 0.035 W, 0.5 W).

Table 3: Final values for the receiver #1

Receiver #1 [W]	0.01	0.035	0.5
<b>Average [V]</b>	0.000523	0.000869	0.001897
<b>Average Power [V<sup>2</sup>]</b>	4.81941e-007	1.34955e-006	6.38660e-006
<b>Avg. noise std. dev. [V]</b>	0.000332	0.000333	0.000335
<b>BER</b>	7.8143e-002	1.5864e-002	1.8121e-004
<b>Q</b>	1.4177e+000	2.1478e+000	3.5660e+000

Fig.11 indicates the eye diagrams for the receiver #2 with input powers EDFA: 0.01 W, 0.035 W, 0.5 W. In Table 4 are the final values for the receiver #2.

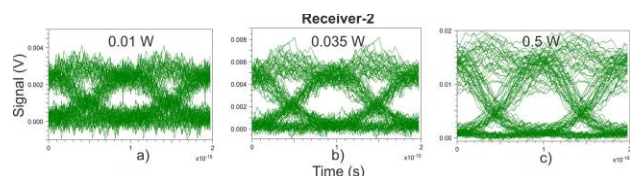


Fig. 11: The eye diagrams for the receiver #2 with powers (0.01 W, 0.035 W, 0.5 W).

Table 4: Final values for the receiver #2

Receiver #2 [W]	0.01	0.035	0.5
Average [V]	0.001225	0.002433	0.006486
Average Power [V <sup>2</sup> ]	2.65080e-006	1.04983e-005	7.71763e-005
Avg. noise std. dev. [V]	0.000334	0.000337	0.000352
BER	7.2143e-004	4.3103e-007	3.6651e-020
Q	3.1859e+000	4.9208e+000	9.1227e+000

In Fig. 12 are shown the eye diagrams for the receiver #3 with EDFA input powers: 0.01 W, 0.035 W, 0.5 W. In Table 5 are the final values for the receiver #3.

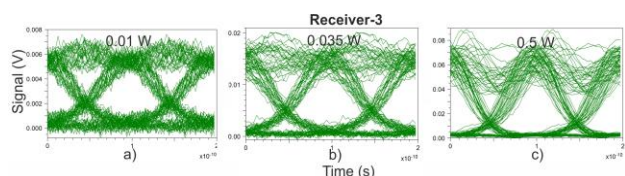


Fig. 12: The eye diagrams for the receiver #3 with powers (0.01 W, 0.035 W, 0.5 W).

Table 5: Final values for the receiver #3

Receiver #3 [W]	0.01	0.035	0.5
Average [V]	0.002767	0.007155	0.026062
Average Power [V <sup>2</sup> ]	0.00276e-005	9.08898e-005	0.001340153
Avg. noise std. dev. [V]	0.000341	0.000360	0.000499
BER	1.4285e-010	6.9670e-035	0.0000e+000
Q	6.3063e+000	1.2265e+001	1.4142e+003

Fig. 13 shows the eye diagrams for the receiver #4 with EDFA input powers: 0.01W, 0.035W, 0.5W. In Table 6 are the final values for the receiver #4

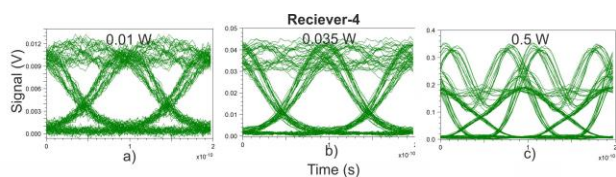


Fig. 13: The eye diagrams for the receiver #4 with powers (0.01 W, 0.035 W, 0.5 W).

Table 6: Final values for the receiver #4

Receiver #4[W]	0.01	0.035	0.5
Average [V]	0.004976	0.017048	0.088577
Average Power [V <sup>2</sup> ]	4.33408e-005	0.000535267	0.017331027
Avg. noise std. dev. [V]	0.000357	0.000440	0.001175
BER	3.2806e-028	4.0797e-197	0.0000e+000
Q	1.0951e+001	2.9929e+001	1.4142e+003

## 5 Conclusion

This article offered the simulation of the four-channel WDM system with the wavelengths of 1566nm, 1562nm, 1558 nm and 1554nm with three pump powers of EDFA (0.01 W, 0.35 W, 0.5 W) with the transmitting speed of 10Gbps. On the input side there were the quantitative parameters of Q and BER evaluated for the respective receivers. With the eye diagrams showed in Fig. #10-13 it is clear that the best results of the eye diagram and error rate parameters are listed in Table 6 for the receiver #4 which operates on the wavelength of 1554 nm. In keeping with the theoretical proposition the error rate and the Q-factor worsen as the wavelength increases.

## References:

- [1] Yamada, M., Ono, H., Kanamori, T., Sudo., Ohishi, Y., Broadband and gain-flattened amplifier composed of a 1.55 $\mu$ m-band and a 1.58 $\mu$ m-band Er<sup>3+</sup>-doped fibre amplifier in a parallel configuration, *Electronics Letters*, Vol. 33, No. 8, 1997, pp.710-711
- [2] Green, P.E., *Fiber to the home*, 2006, ISBN-13: 978-0471742470, 139 pp.
- [3] Turán, J., Ovseník, L., Filo, P., Turán Jr., J., Fazekas, K., Multimedia courseware: Applied photonic, *Video/Image Processing and Multimedia Communication*, Vol. 2, 2003, pp.741-746.
- [4] Zhang, S.L.; Lane, P.M.; O'Reilly, J.J., Effect of EDFA ASE noise on the performance of millimetre-wave fibre radio communication systems, *Microwave Photonics*, Vol. 5, No.5, 1996, pp. 149-152.

- [5] Lee, W.L., Min, B., Ahn, S., Park, N., Simulation for the effect of cascaded gain-temperature dependence on 40 channel-50 EDFA WDM link under temperature fluctuations, *Lasers and Electro-Optic*, Vol.3, 1999, pp. 646-647.
- [6] Becker, C.P., Olsson, N.A., Simpson, J.R., *Erbium-Doped Fiber Amplifier*, 1999, ISBN 0-12-084590-3, 481 pp.
- [7] Turán, J., Ovseník, L., Experimental free space optics project, *15th International Workshop on ADC Modelling and Testing, and 3rd Symposium IMEKO TC19 - Environmental Measurements*, 2010, pp.431-434.
- [8] Zyskind, J., Srivastava, A., *Optically Amplified WDM Networks*, 2010, ISBN-13: 978-0123749659, 512 pp.
- [9] Khaleghi, F.; Li, J.; Kavehrad, M.; Kim, H., Increasing repeater span in high-speed bidirectional WDM transmission systems using a new bidirectional EDFA configuration, *Photonics Technology Letters*, Vol. 8, No.9, 1996, pp.1252-1254.
- [10] Ivaniga, T., Ivaniga, P., Evaluation of the bit error rate and Q factor in optical networks, *IOSR Journal of Electronics and Communication Engineering*, Vol.9, No.6, 2014, pp.01-03.
- [11] Mukherjee, P.P., Sarkar, S., Das, N.R., A comparative study on determination of optimum detection threshold for minimum BER in a WDM receiver with component crosstalk, *Microwave and Photonic*, Vol.1, No. 4, 2013, pp. 13-15.
- [12] Ghatak, A., Thyagarajan, K., *FIBER OPTIC ESSENTIALS*, 2007, ISBN 978-0-470-09742-7, 259 pp.
- [13] Ferreira, S.F.M., *NONLINEAR EFFECTS IN OPTICAL FIBERS*, 2011, ISBN 978-0-470-46466-3, 376 pp.
- [14] Ovseník, L., Turán, J., Tatarko, M., Turan, M., Vásárhelyi, J., Fog sensor system: Design and measurement, *Proceedings of the 2012 13th International Carpathian Control Conference*, Vol. 28, No. 31, 2012, pp. 529-532.
- [15] Shake, I., Takara, H., Kawanishi, S., Simple Q factor monitoring for BER estimation using opened eye diagrams captured by high-speed asynchronous electrooptical sampling, *Photonics Technology Letters*, Vol.15, No.4, 2003, pp.620-622.
- [16] Ivaniga, T., Overview of Degradation Mechanism in All-Optical WDM Systems, *15th Scientific Conference of Young Researchers : proceedings from conference : May 19th, 2015, Herľany, Slovakia*, 2015, ISBN 978-80-553-2130-1, pp.80-83.
- [17] Ramaswami, R., Sivarajan K.N., Sasaki, H.K., *Optical Networks A principle Perspective (Third Edition)*, 2010, ISBN: 978-0-12-374092-2, 928 pp.
- [18] ITU-T.G.652 – “Characteristics of a single-mode optical fibre and cable”, [online],[cit. 08.07.2015]. ITU-T, November 2009. Available on the internet: <http://www.itu.int/rec/T-REC-G.652-200911-I>.
- [19] Tatarko, M., Ovseník, L., Turan, J., Properties of hybrid FSO/RF link with 60 GHz RF backup link, *Information & Communication Technology Electronics & Microelectronics (MIPRO), 2013 36th International Convention on*, Vol. 20, No. 24, 2013, pp. 495-497.
- [20] Ivaniga, P., *Hodnocení chybovosti ve vysokorychlostných digitálných sítich*, 2007, ISBN: 978-80-8070-771-2, 78 pp.
- [21] Bousselet, P., Lanne, S., Thiry, J.P., Frignac, Y., Lepingard, F., Simonneau, C., Corbel, E., Bayart, D., Hamaide, J.-P., Agostini, E., Nowodzinski, A., BER validation of ring-doping cladding-pumped EDFAs for dense WDM applications, *Electronics Letter*, Vol. 38, No.11, 2002, pp. 522-523.
- [22] Agrawal, G.P., *Nonlinear Fiber Optics (Fifth Edition)*, 2013, ISBN: 978-0-12397-023-7, 621 pp.
- [23] Srivastava, M., Kapoor, V., Analysis and compensation of self phase modulation in wavelength division multiplexing system, *Engineering and Systems (SCES), 2014 Students Conference*, vol.1, no.4, 2014, pp. 28-30.